Rare Met. (2013) 32(3):305–311
DOI 10.1007/s12598-013-0060-y

RARE METALS
www.editorialmanager.com/rmet

Current efficiency in electro-winning of lanthanum and cerium metals from molten chloride electrolytes

Deepak Kumar Sahoo*, Harvinderpal Singh, Nagaiyar Krishnamurthy

Received: 9 November 2012 / Revised: 4 December 2012 / Accepted: 15 December 2012 / Published online: 7 June 2013

Abstract The objective of this study is to prepare lanthanum and cerium metals by fused salt electrolysis of their anhydrous chloride in molten media such as LiCl–KCl, NaCl–KCl, KCl, NaCl, and LiCl and to characterize the metal deposit by X-ray diffraction, energy dispersive X-ray fluorescence, and inductive coupled plasma-atomic emission spectroscopy. Deposit metal of purity more than 99 % was obtained in each of the experiments. The entire process starting from preparation of anhydrous lanthanum/cerium chloride to electrolysis yielding of metal deposits has been described. The effect of process parameters such as temperature, electrolyte composition, and current density on the current efficiency was studied. All these parameters were varied to get the highest current efficiency and metal yield. The major non-rare earth impurities with the deposit are found to be Fe, Cr, and Ni along with $\sim 1 \times 10^{-3}$ of total gaseous impurities.

Keywords Fused salt electrolysis; Current density; Current efficiency; Rare earths

1 Introduction

Rare earth metals possess some unique physical and metallurgical properties that make them valuable functional materials in devices for electronic, magnetic, superconductor, and hydrogen storage applications [1–4]. Rare earth metals impart desirable mechanical and corrosion resistance properties in a number of ferrous and nonferrous metals and alloys [5–7]. Cerium and lanthanum are the most abundant rare earth elements available in the ores of monazite and bastenite. These metals are very reactive and they form very stable oxides. A wide variety of precursors ranging from oxides to chlorides and fluorides are used in preparing these metals. Due to the strong electropositive character of these metals, chemical reduction with the common reducing agents is not possible. Strong reducing agents such as calcium is required for oxide and for halides, calcium and lithium are effective. Therefore, the practical methods for preparation of these metals are limited to techniques such as calciothermic reduction and electro-winning. Fused salt electrolysis process for making these metals is attractive because of low cost, ease of operation, batch size, and the purity of the product. Moreover, fused salt electrolysis becomes particularly attractive for these (La and Ce) metals, because their melting point facilitates their electro-winning in molten state, which eventually yields a product with minimum contamination. Various investigations have been reported for electro-winning of lanthanum and cerium in both chloride and fluoride baths [8–12]. Although fluoride salt is stable in air compared with chloride, which is hygroscopic, the advantages of chloride are ease of preparation and low-melting temperature.

The carrier electrolytes used in this process are mostly alkali and alkaline halides, which have good solubility for rare earth metal halides. The low hygroscopicity of alkali halides makes them more favored over alkaline halides. LiCl–KCl and NaCl–KCl are the most common flux used for this purpose [13]. In this process, various factors

D. K. Sahoo*, H. Singh
Rare Earths Development Section, Bhabha Atomic Research Centre, Trombay, Mumbai 400085, India
e-mail: deesahoo@gmail.com

N. Krishnamurthy
Fusion Reactor Materials Section, Bhabha Atomic Research Centre, Trombay, Mumbai 400085, India

including temperature, current density (for both cathode and anode), and duration of electrolysis can affect the outcome of the product. However, data on the effects of temperature, bath composition, duration, and current densities are limited in the literature. The objective of this study is to observe the effect of process parameters in LiCl–KCl and NaCl–KCl baths and to investigate the effect of using single carrier electrolyte such as KCl, NaCl, and LiCl in preparing lanthanum and cerium metals.

2 Experimental

The starting materials used lanthanum and cerium oxides (>99 % pure) obtained from Indian Rare Earths Ltd. Potassium chloride, sodium chloride, and lithium chloride having 99.5 % purity of LR grade were procured from the local market. Molybdenum rod of 99 % purity and high-density graphite ($\rho = 1.82 \times 10^3$ kg·m^{-3}) crucibles were used as cathode and anode, respectively.

The first step in the overall process is the conversion of La/Ce oxides to their corresponding chlorides. The oxides were dissolved in hot hydrochloric acid (50 % strength) with constant stirring until the crystallization occured [14]. The temperature of the solution was maintained within 353–373 K. The product obtained was examined by X-ray diffraction (XRD) analysis and found to be La/$CeCl_3 \cdot 7H_2O$. Dehydration of $LaCl_3 \cdot 7H_2O$ was carried out by stepwise heating to 523 K for 24 h in dynamic vacuum and the escaping water vapor was collected by using a liquid nitrogen trap. Mixture of LiCl–KCl (in 1:1 weight ratio) was also dehydrated at 523 K for 4 h to remove adsorbed moisture. The mixture of anhydrous $LaCl_3$ with LiCl–KCl taken in a required proportion was used as electrolyte for lanthanum metal deposition. Experiments were also conducted in NaCl–KCl bath in place of LiCl–KCl flux. The electrolytic mixture taken in each experiment was 1 kg with different concentrations of $LaCl_3$, keeping the weight ratio of LiCl/NaCl:KCl constant (i.e., 1:1). Similar experiments were carried to electro-win cerium metal from $CeCl_3$ using LiCl–KCl and also with NaCl–KCl carrier electrolyte separately.

The electrolytic mixture was charged into a 0.7 m diameter and 0.25 m tall graphite crucible, which served the purpose of container material as well as anode. A molybdenum rod of 0.6 mm diameter used as cathode was sheathed by a close-fitting alumina tube stuffed with asbestos rope, except the portions required to see the electrolyte in the lower part and for cathode connection in the upper part. The role of alumina sheath was to give electrical insulation and also to prevent molybdenum rod from getting corroded with Cl_2 gas, which forms during electrolysis. A schematic diagram of the electrolytic cell assembly is shown in Fig. 1. It consists of a vacuum tight Inconel retort (0.1 m diameter) fitted with a stainless steel flange system having provision for placing the cathode rod and thermocouple and for gas inlet and outlet. The negative terminal of DC power supply is connected to Mo rod and positive terminal to Inconel retort, which eventually makes graphite as anode. To collect the material deposited at cathode, an alumina crucible was placed below the cathode inside the graphite crucible. The alumina crucible and cathode rod were kept in such a manner that the tip of the molybdenum rod was just above the alumina crucible. The graphite crucible was placed in the Inconel retort, which was kept in a tubular vertical resistance furnace as shown in Fig. 1. The resistance furnace with temperature electronic control (±1 K) was used to heat the cell up to the operating temperature. The electrolyte in the graphite crucible was melted in high pure argon gas. The role of argon gas is also to prevent the oxidation of cell material. The temperature of the bath was measured with a K-type thermocouple protected by an alumina well inserted into the melt. After equilibrating the bath for 1 h, the cathode was lowered and pre-electrolysis was carried out to remove residual water followed by electrolysis applying potential of 5–8 V from a DC power supply. Electrolysis was continued for a specific period of time, and after electrolysis, the cell was allowed to cool to room temperature in an argon atmosphere. Molybdenum rod and thermocouples were taken above the electrolytic bath to prevent them from sticking inside the salt, which solidifies on cooling. The molten metal collected in the alumina crucible was recovered by washing solidified molten salt with water. The alumina being nonconducting helped to protect the metal from anodic attack, as well as reaction with graphite crucible. The amount of metal collected in each experiment was 0.2–0.3 kg according to the amount of functional electrolyte.

Similar experiments were also carried out using only one solvent such as KCl, LiCl, and NaCl to study effect of

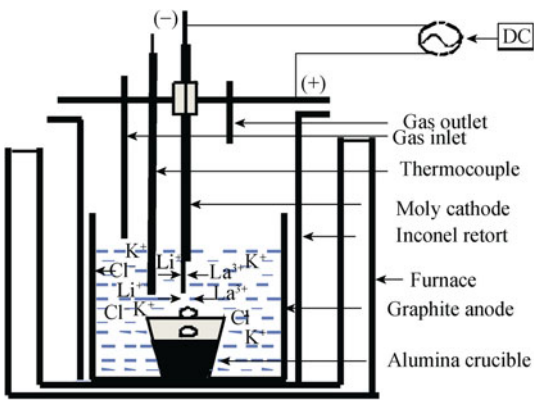

Fig. 1 Scheme of electrolyte cell

change in carrier electrolyte on the process and yields. Products were analyzed by X-ray diffraction (XRD), energy dispersive X-ray fluorescence (EDXRF), and inductive coupled plasma-atomic emission spectroscopy (ICP-AES).

3 Results and discussion

3.1 Electrolytic reaction

The cell can be represented as follows:

$$\mathrm{C\ (graphite)}, \mathrm{Cl_2(gas)}|\mathrm{LaCl_3 - LiCl - KCl}|\mathrm{La^{3+}/La, Mo}$$

$$\text{At cathode (Mo)},\ \mathrm{La^{3+} + 3e^- \rightarrow La}$$

$$\text{At anode (graphite)}, \mathrm{3Cl^- \rightarrow 3/2Cl_2 + 3e^-}$$

3.2 Characterization of metal

In the first step, the lanthanum and cerium metal products were characterized by XRD. Figures 2 and 3 show the XRD pattern of cerium and lanthanum metals. All the diffracted peaks well match with their corresponding PCPDF patterns of 36-0815 and 78-0638, respectively. No diffraction from any impurities is found, indicating the impurities below X-ray detection limit.

EDXRF patterns of cerium and lanthanum metals are shown in Figs. 4 and 5. From these spectra, it is clearly observed that the major peaks belong to lanthanum and cerium metals, with some peaks of other elements such as Ni, Cr, and Fe.

Chemical analysis results given in Table 1 show the quantitative picture of metal purity. From Table 1, it is clearly observed that the metal purity obtained in each experiment is more than 99 %. The iron, chromium, and nickel impurities vary from 0.1 wt% to 0.3 wt%. The chromium impurity mostly comes from molybdenum cathode, which contains ~0.5 wt% chromium. The impurities of iron and nickel probably come from the salt mixture of alkali chlorides. By using higher purity chemicals and electrodes, it is probably possible to get these metals in higher purity state. The gaseous

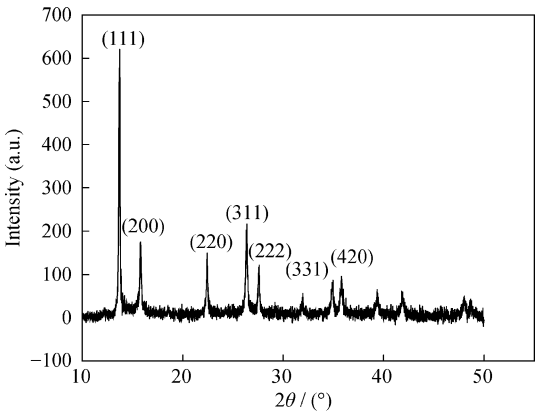

Fig. 2 XRD pattern of electrodeposited Ce metal

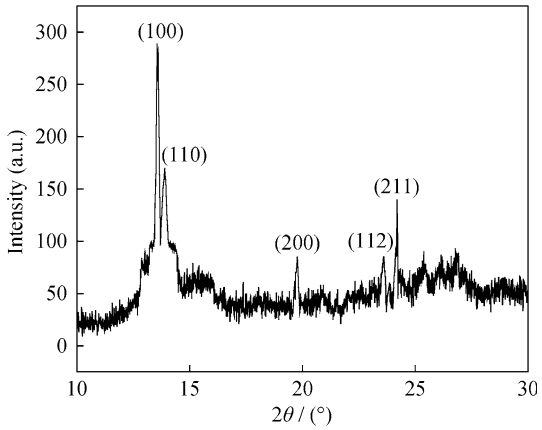

Fig. 3 XRD pattern of electrodeposited La metal

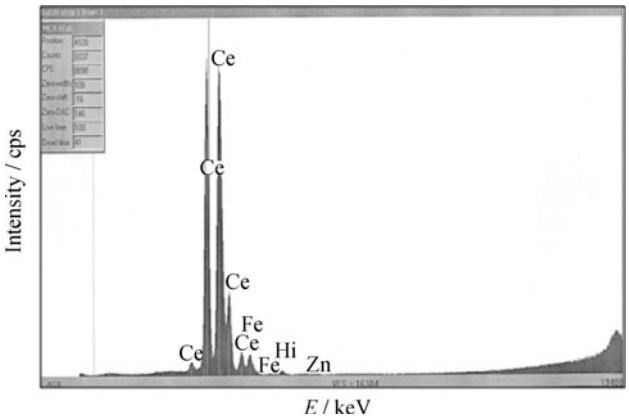

Fig. 4 EDXRF pattern of electrodeposited Ce metal

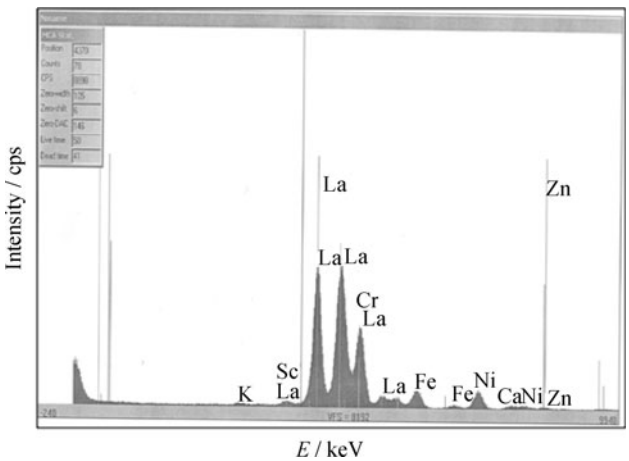

Fig. 5 EDXRF pattern of electrodeposited La metal

Table 1 Evaluation of metal purity

Metals	Electrolytic bath	Purity/%	Elemental impurities/%							Gaseous impurities/%		
			Fe	Ni	Cr	C	K	Na	Li	Oxygen	Nitrogen	Hydrogen
La	NaCl–KCl	99	0.5	0.3	0.05	0.01	0.016	0.020		0.005	0.001	0.01
Ce	NaCl–KCl	99	0.3	0.5	0.10	0.01	0.015	0.016		0.006	0.002	0.01
La	LiCl–KCl	99	0.4	0.3	0.05	0.01	0.012		0.010	0.008	0.002	0.01
Ce	LiCl–KCl	99	0.3	0.3	0.05	0.01			0.010	0.006	0.003	0.01
La	KCl	99	0.5	0.3	0.03	0.01	0.040			0.005	0.001	0.01
Ce	KCl	99	0.3	0.5	0.05	0.01	0.050			0.006	0.002	0.01
La	NaCl	99	0.4	0.3	0.04	0.01		0.050	0.010	0.008	0.002	0.01
Ce	NaCl	99	0.3	0.3	0.05	0.01		0.060	0.010	0.006	0.003	0.01
La	LiCl	99	0.3	0.4	0.04	0.01			0.008	0.006	0.001	0.01
Ce	LiCl	99	0.4	0.5	0.05	0.01			0.008	0.002	0.001	0.01

impurities of hydrogen, nitrogen, and oxygen are found in 1×10^6 level. These impurities may be avoided by using high-pure argon gas as protective atmosphere instead of commercial grade of argon as used in our experiments.

3.3 Relation between electrolytic temperature and current efficiency

The effect of temperature on current efficiency (CE) is shown in Figs. 6 and 7. Metals were obtained by electrolysis in the electrolytic bath containing 40 wt% $LaCl_3$/$CeCl_3$ with equimolar ratio of NaCl and KCl. All these experiments were carried out at a constant current density of 1×10^5 A·m^{-2} for 3 h. From Fig. 6, it is clearly seen that, with the increase of electrolysis temperature, current efficiency for cerium metal increases and reaches maximum value and thereafter started falling. Owing to high viscosity of electrolyte at lower temperature electrical conductivity, and mobility of ions is low at low temperature, the diffusion movement electro-active species is slow, which is unfavorable in improving the current efficiency. With the increase of temperature, increased diffusion kinetics gives higher current efficiency. However, after a certain optimum temperature, the current efficiency begins to decrease due to increased solubility of cathode deposit in the melt [15], as well as higher volatilization of the electrolyte. The optimum temperature for electro-winning of cerium is 1,163 K. In the case of lanthanum, the operational temperature is high, as its melting point of 1,194 K is higher than that of cerium, whose melting point is 1,080 K. Owing to high operational temperature, CE is maximum due to enhanced diffusion kinetics of lanthanum ion. On further increase in temperature, efficiency decreases due to increase in solubility of metal in the melt. The optimum temperature for lanthanum deposition is found to be 1,213 K.

3.4 Effect of concentration of functional electrolyte on CE

The effect of change in concentration of La/$CeCl_3$ on CE is shown in Fig. 8. Here, the mass fraction of $LnCl_3$ varies under a cathode current density (CCD) of 7×10^4 A·m^{-2}. Operating temperature for lanthanum and cerium were 1,213 and 1,163 K, respectively. At low concentration of functional electrolyte, CE is low due to preferential reduction of solvent ions compared with functional ions according to Nernst equation. With increase in concentration, CE starts increasing due to availability of more lanthanide ions around cathode. This is substantiated by observing improvement in CE by increasing concentration of $RECl_3$ in the electrolyte up to 50 wt%. Further increase in the concentration of metal chloride makes the bath more viscous, which decreases the conductivity of molten electrolyte and hence decreases the CE. Therefore, the optimum concentration of $LnCl_3$ in both lanthanum and cerium cases appears to be 50 wt%. It is evident from the Fig. 8 that CE for cerium metal is lower than that of lanthanum metal. Cyclic oxidation and reduction between Ce(III) and Ce(IV) are presumed to be the reason for low CE in cerium [9].

3.5 Effect of CCD on CE

The relationship between CCD and CE was studied for both La and Ce metal deposition in LiCl–KCl and NaCl–KCl baths. Figure 9 shows the variation of CE in the CCD range of $(4–10) \times 10^4$ A·m^{-2} for both $LaCl_3$–NaCl–KCl and $LaCl_3$–LiCl–KCl. Similarly, Fig. 10 shows the variation of CE in the CCD range of $(4–16) \times 10^4$ A·m^{-2} both for $CeCl_3$–NaCl–KCl and $CeCl_3$–LiCl–KCl. The $LnCl_3$ content in each case is 50 wt%. Operational temperature for cerium is 1,163 K and that of lanthanum is 1,213 K.

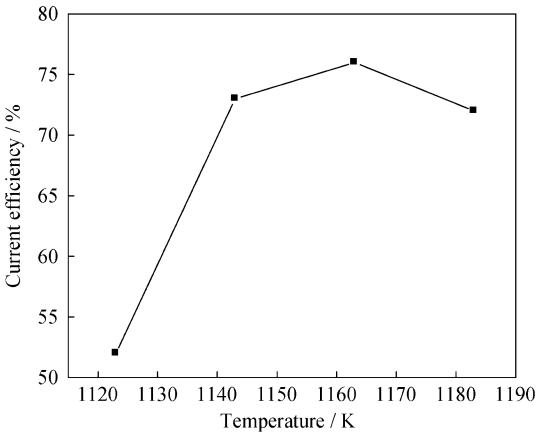

Fig. 6 CE at different temperatures of operation for Ce metal

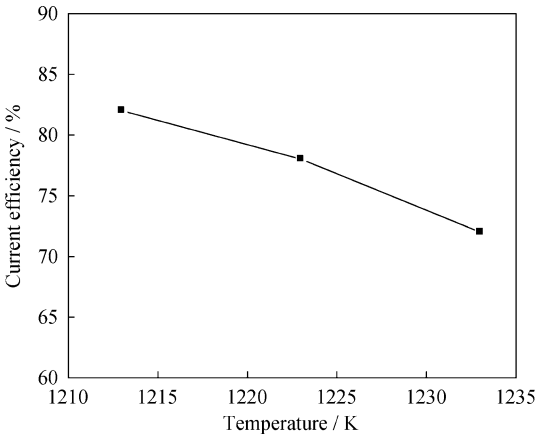

Fig. 7 CE at different temperatures of operation for La metal

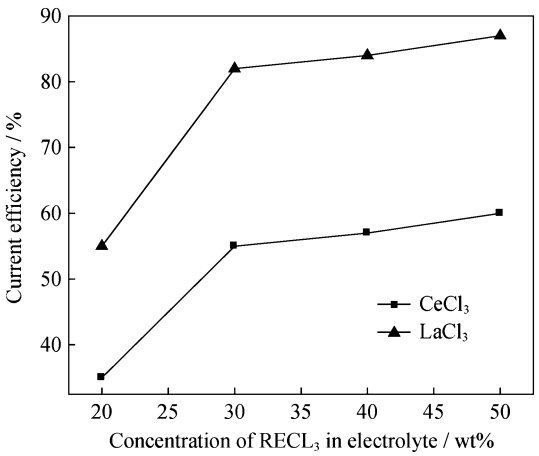

Fig. 8 Effect of concentration of $RECl_3$ on CE

Both Figs. 9 and 10 show that CE increases with the increase of CCD. On increasing the current density, the kinetics of migration of lanthanide ions increases due to the increase of cathodic potential, which helps in depositing

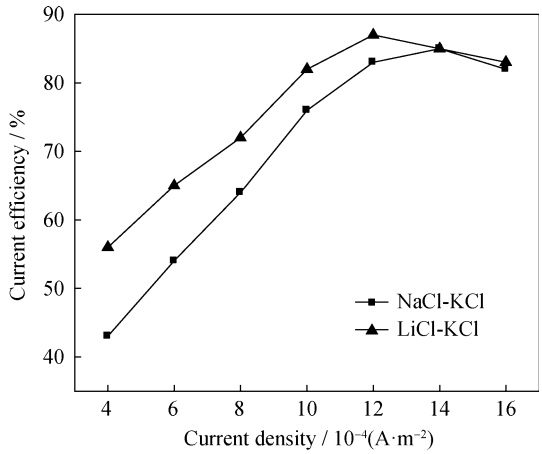

Fig. 9 Influence of current densities on CE for Ce metal in LiCl–KCl and NaCl–KCl flux

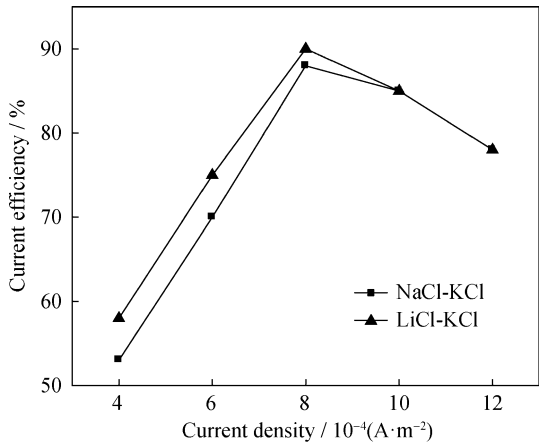

Fig. 10 Influence of current densities on CE for La metal in LiCl–KCl and NaCl–KCl flux

metals at a greater speed and thus increases the CE. However, a very high-current density results in the co-deposition of flux ions due to high-negative potential of cathode, which reaches the deposition potential of flux ions. The optimum CCD for lanthanum deposition is 8×10^4 A·m^{-2} in both LiCl–KCL and NaCl–KCl melts. For cerium, the optimum CCD is 10×10^4 A·m^{-2} in LiCl–KCl melt and 12×10^4 A·m^{-2} in NaCl–KCl melt.

3.6 Effect of changing the carrier electrolyte

Figures 9 and 10 give the comparison picture of effect of CCD on CE for both metals in LiCl–KCl and NaCl–KCl solvents. The range of stability and greater fluidity of LiCl–KCl over NaCl–KCl solvent shows the CE trend in Figs. 9 and 10. It is found that, at lower current density, there may be a significant difference in CE, but at higher current density this difference is negligible. At lower current density, CE for cerium metal, in particular, is low, which

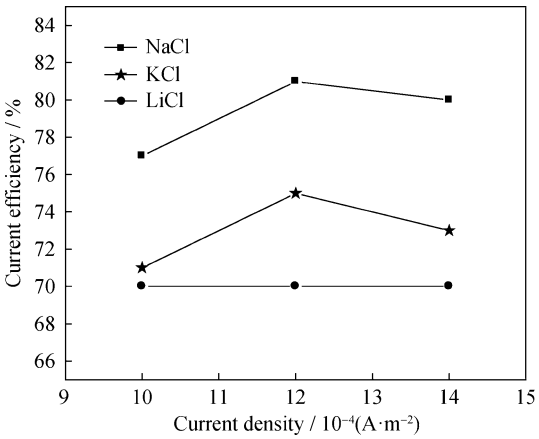

Fig. 11 Variation of CE on using individual flux for cerium metal

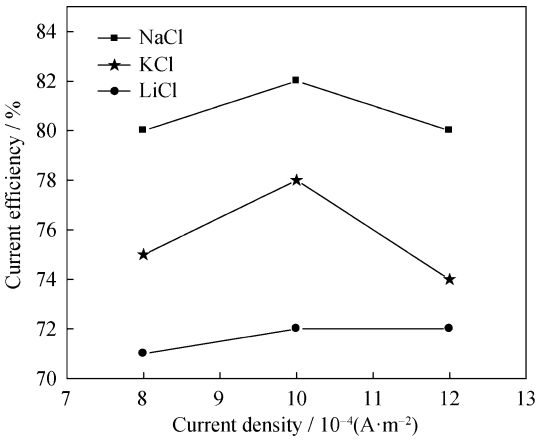

Fig. 12 Variation of CE on using individual flux for lanthanum metal

may be attributed to cyclic oxidation and reduction of Ce^{3+} and Ce^{4+}. This is contradictory to the Ref. [16], which reported that reduction of Ce(III) to Ce(0) was a single-step process. Low CE for Ce at low CCD could be due to low-internal mobility of cerium ion compared with lanthanum ion [17]. The increase of mass transfer rate at a higher current density leads to higher CE values for both LiCl–KCl and NaCl–KCl baths. From the industrial production point of view, NaCl–KCl has the advantage over LiCl–KCl due to its low cost.

The preparation of metals is also possible using only individual flux such as KCl, NaCl, or LiCl. In these cases, applied voltage in the electrolysis is slightly higher than the LiCl–KCl or NaCl–KCl flux. The CEs obtained in these cases are comparable with that obtained in mixture solvent. The purity of metal and amount of flux metal obtained here is also comparable with that of prepared in mixed solvent as evident from Table 1. Another interesting factor is found here: CE decreases from KCl to NaCl and to LiCl for both metals as shown in Figs. 11 and 12. Although this trend is not fully understood, it is believed to be due to the slow mass transfer of lanthanide ions in NaCl and LiCl compared with KCl melt. It could be due to the formation of higher-order lanthanide complex in the presence of NaCl and LiCl [18–23]. Further studies are definitely required to predict the mechanism for this observed trend.

4 Conclusion

Cerium and lanthanum metals with more than 99 % purity were prepared in batches of 0.3 kg each. All the process parameters were varied to get high CE and yield for both these metals in LiCl–KCl and NaCl–KCl baths. CE of 87 % and 90 % are obtained in preparing Ce and La metal, respectively, by operating the electrolytic cell under best conditions. The suitable temperature for electro-winning of cerium and lanthanum is found to be 1,163 and 1,213 K, respectively. The optimum CCD for lanthanum deposition is 8 $A{\cdot}cm^{-2}$ in both LiCl–KCL and NaCl–KCl melts. For cerium, the optimum CCD is 10 $A{\cdot}cm^{-2}$ in LiCl–KCl melt and 12 $A{\cdot}cm^{-2}$ in NaCl–KCl melt. Preparations of these metals were also carried out using individual flux of KCl, LiCl, and NaCl. Maximum CE and yield were observed in KCl compared with NaCl or KCl flux for both the metals.

References

[1] Chakoumakus Bryan C, Sales Brian C, Mandrus David, Keepens Veerle. Disparate, atomic displacements in skutterudite-type $LaFe_3CoSb_{12}$, a model for thermoelectric behavior. Acta Crystallogr B. 1999;B55(3):341.
[2] Sarkis Angie, Callen Earl. Magnetic anisotropy of rare earths-transition metal compounds. Phys Rev B. 1982;26(7):3870.
[3] Soto F, Cabo L, Mosqueira J, Ramallo MV, Veira JA, Vidal F. Observation of enhanced fluctuation of diamagnetism in lanthanum superconductors with dilute magnetic impurities. Europhys Lett. 2006;73(4):587.
[4] Konishi H, Yoshihara Y, Ono H, Usui T, Oishi T, Nohira T. Electrochemical formation and phase control of La–Ni alloy films in LiCl–KCl melts. J Jpn Soc Exp Mech. 2010;10(SI):215.
[5] Jain C-C, Koo C-H. Creep and corrosion property of the extruded magnesium alloy containing rare earth. Mater Trans. 2007;48(2):265.
[6] Fukumoto M, Yamashita R, Hara M. Improvement in oxidation resistance of stainless steel by molten salt electrodeposition of La. Oxid Met. 2004;62(5–6):309.
[7] Hughes AE, Gorman JD, Paterson PJK. Characterization of Ce–Mo based conversion coatings on Al alloys. Corros Sci. 1996;38(11):1957.
[8] Yamamura T, Mehmood M, Maekawa H, Sato Y. Electrochemical processing of rare-earth and rare metals by using molten salts. Chem Sustain Dev. 2004;12(1):5.
[9] Singh S, Pappachan AL, Gadiyar HS. Electrodeposition of cerium and Ce–Co alloy. J Less Common Met. 1968;120(2):307.
[10] Singh S, Pappachan AL. Electrowinning of cerium group metal from fused chloride bath. Bull Mater Sci. 1980;2(3):155.

[11] Constantin V, Popescu AM, Zuca S, Gaune-Escard M, Olteanu M. Electrochemical studies on cerium(III) in molten fluoride mixture. J Rare Earths. 2010;28(3):428.
[12] Kaneko A, Yamamoto Y, Okada C. Electrochemistry of rare earth fluoride molten salt. J Alloys Compd. 1993;193(1–2):44.
[13] Gupta CK, Krishnamurthy N. Extractive metallurgy of rare earths. Int Mater Rev. 1992;37(5):197.
[14] Gaune-Escard M, Bogacz A, Rycerz L, Szczepaniak W. Heat capacity of $LaCl_3$, $CeCl_3$, $PrCl_3$, $NdCl_3$, $GdCl_3$, $DyCl_3$. J Alloys Compd. 1996;235(2):176.
[15] Feng L, Guo C, Tang D. Relation between the dissolution behavior and current efficiencies of La, Ce, Pr and Nd in their chloride molten salts. J Alloys Compd. 1996;234(2):183.
[16] Castrillejo Y, Bermejo MR, Pardo R, Martinez AM. Use of electrochemical techniques for the study of solubilization of cerium-oxide compounds and recovery of metal from molten chlorides. J Electroanal Chem. 2002;522(2):124.
[17] Zablocka-Malicka M, Szczepaniak W. Internal mobility of Ln^{3+} ions in KCl–$LnCl_3$ and NaCl–$NdCl_3$ systems. A single coefficient correlation model. J Mol Liq. 2008;137(1–3):36.
[18] Matsumiya M, Seo K. A molecular dynamics simulation of the transport properties of molten ($La_{1/3}$, K)Cl. Z J Nat Res A. 2005;60:187.
[19] Kushkhov KhB, Vindizheva MK, Karashaeva RA. Electroreduction of cerium ions on silver electrode in halide melts at 973 K. Russ J Electrochem. 2006;42(8):830.
[20] Photiadis GM, Borresen B, Papatheodorou GN. Vibrational modes and structures of lanthanide halide–alkali halide binary melts. J Chem Soc Faraday Trans. 1998;94:2605.
[21] Okamoto Y, Shiwaku H, Yaita T, Narita H, Tanida H. Local structure of molten $LaCl_3$ by K-absorption edge of XAFS. J Mol Struct. 2002;641:71.
[22] Mukherjee A, Gulnar AK, Sahoo DK, Krishnamurthy N. Gas solid techniques for preparation of pure lanthanum hexaboride. Rare Met. 2012;31(3):285.
[23] Wang N, Huang K, Hou J, Zhu H. Preparation of niobium nanoparticles by silicothermic reduction of Nb_2O_5 in molten salts. Rare Met. 2012;31(6):621.